ACCOUNTS
of chemical research

Article

pubs.acs.org/accounts

Paradigms and Challenges for Bioapplication of Rare Earth Upconversion Luminescent Nanoparticles: Small Size and Tunable Emission/Excitation Spectra

Ling-Dong Sun,* Ye-Fu Wang, and Chun-Hua Yan*

Beijing National Laboratory for Molecular Sciences, State Key Laboratory of Rare Earth Materials Chemistry and Applications & PKU-HKU Joint Laboratory in Rare Earth Materials and Bioinorganic Chemistry, College of Chemistry and Molecular Engineering, Peking University, Beijing 100871, China

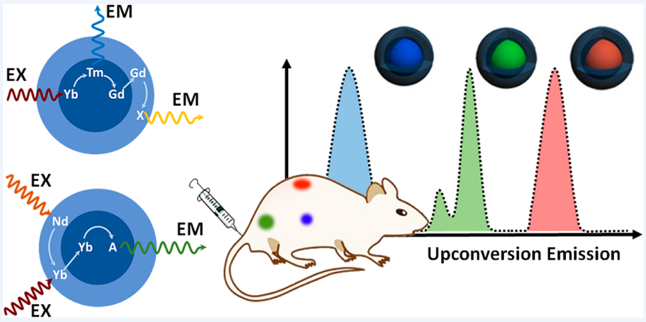

CONSPECTUS: Rare earth (RE) materials, which are excited in the ultraviolet and emit in the visible light spectrum, are widely used as phosphors for lamps and displays. In the 1960's, researchers reported an abnormal emission phenomenon where photons emitted from a RE element carried more energy than those absorbed, owing to the sequential energy transfer between two RE ions—Yb^{3+}-sensitized Er^{3+} or Tm^{3+}—in the solid state. After further study, researchers named this abnormal emission phenomenon upconversion (UC) emission. More recent approaches take advantage of solution-based synthesis, which allows creation of homogenous RE nanoparticles (NPs) with controlled size and structure that are capable of UC emission. Such nanoparticles are useful for many applications, especially in biology. For these applications, researchers seek small NPs with high upconversion emission intensity. These UCNPs have the potential to have multicolor and tunable emissions via various activators. A vast potential for future development remains by developing molecular antennas and energy transfer within RE ions. We expect UCNPs with optimized spectra behavior to meet the increasing demand of potential applications in bioimaging, biological detection, and light conversion.

This Account focuses on efforts to control the size and modulate the spectra of UCNPs. We first review efforts in size control. One method is careful control of the synthesis conditions to manipulate particle nucleation and growth, but more recently researchers have learned that the doping conditions can affect the size of UCNPs. In addition, constructing homogeneous core/shell structures can control nanoparticle size by adjusting the shell thickness. After reviewing size control, we consider how diverse applications impose different requirements on excitation and/or emission photons and review recent developments on tuning of UC spectral profiles, especially the extension of excitation/emission wavelengths and the adjustment and purification of emission colors. We describe strategies that employ various dopants and others that build rationally designed nanostructures and nanocomposites to meet these goals. As the understanding of the energy transfer in the UC process has improved, core/shell structures have been proved useful for simultaneous tuning of excitation and emission wavelengths. Finally, we present a number of typical examples to highlight the upconverted emission in various applications, including imaging, detection, and sensing. We believe that with deeper understanding of emission phenomena and the ability to tune spectral profiles, UCNPs could play an important role in light conversion studies and applications.

1. INTRODUCTION

Rare earth (RE)-ion-doped nanomaterials with upconversion (UC) emission are a unique type of phosphor. In a typical UC process, two or more low-energy near-infrared (NIR) photons could be converted into a high-energy one, which is located in the ultraviolet (UV), visible (vis), or NIR region.[1] During the first decades after its discovery in 1960's, UC materials have been widely studied in solid laser and display device applications.[2] With the development in fabrication and characterization techniques, the past decade witnessed the rapid advancement of research on upconverting nanomaterials.[3] Plenty of interest has been devoted to this field, attracted by the potential in a variety of applications, including sensing, imaging, and photoactivated therapy.[4]

RE-ion-doped UC nanoparticles (NPs) are favored for various reasons. First, they feature large anti-Stokes shifts, which are barely observed in naturally occurring fluorophores. The NIR excitation results in minimal autofluorescence background, promising a high signal-to-noise ratio (SNR) in biological sensing and imaging studies.[5] Second, the excitation wavelength (usually 980 nm) locates within the so-called "biological window", promising low photodamage and high penetration depth for in vivo applications.[6] Third, these UCNPs possess high photostability and chemical stability, and they barely show any photobleaching and blinking.[7] Last

Received: September 6, 2013
Published: January 14, 2014

but not least, with proper surface modification and functionalization, UCNPs show good biocompatibility, and no evidence yet suggests noticeable biotoxicity, neither in vitro nor in vivo.[8,9]

Nevertheless, there still exist great challenges yet to be addressed. Generally, these challenges arise from the nature of f–f transitions of RE ions and are exacerbated by the small particle size. Essentially, the principle-forbidden f–f transitions result in small absorption cross section of RE ions, hence limiting the excitation efficiency of the UC process. In most cases, RE ions with relatively larger absorption cross sections (usually Yb^{3+}) are introduced as sensitizers. However, the small absorption cross sections of UCNPs are still a bottleneck for obtaining intense UC emissions. Lasers are usually required to produce intense UC emissions. Improvement of UC emission behavior has always been a major concern in this research field.

Furthermore, defects and ligands on the particle surface could quench the excited RE ions nearby. This effect becomes more pronounced as the particle size becomes smaller, dissipating a considerable part of the excitation energy into vibrations of surface defects and ligands. Although large NPs with relatively small surface area are complementary to this issue, larger particles are less favored when mobility and metabolic toxicity are considered for biological applications. Therefore, enhancing the UC emission while simultaneously controlling the particle size is of great importance.

The ladder-like energy states and the shielding effect of 4f electrons further pose restrictions on the excitation and emission wavelengths for UCNPs. The emission wavelengths are essentially determined by the activators. As only a few ions are available as effective activators, there are limited choices for emission bands. Meanwhile, a single type of activator could give multiple emission bands, further complicating the emission selection and multiplex detections. Highly selective and energy-economical methods for emission color modulation are thus required.

The excitation wavelength depends on the rare-earth sensitizers for UC emissions. Yb^{3+} ions, commonly used as effective sensitizers, give an efficient excitation band around 980 nm. Such narrow-band excitation is insufficient to convert the solar energy from a wide NIR wavelength region. Furthermore, the absorption of water at 980 nm could cause a non-negligible tissue heating effect, which might pose a risk for in vivo applications.

With such issues in research, here we will discuss the strategies and the latest progress in realizing small particles with tunable emissions and excitation. We will also address the performances of these small, bright UCNPs with designed spectral features in various types of applications.

2. SIZE CONTROL OF UCNPS

While a small and compact structure is always desirable for in vivo nanoprobes, it has been a great challenge to simultaneously maintain or enhance the UC emission intensity while reducing the size. The key point is to avoid the quenching from the surface quencher accompanying the small particle. Different strategies are available to obtain highly crystallized small NPs with a thermodynamically stable phase or to build core/shell nanostructures for isolating luminescent centers from surface quenchers.

2.1. Doping-Induced Size Transition

With the development of new synthesis routes and novel host materials, many studies have reported obtaining sub-10 nm UCNPs.[10−12] Generally, these achievements are realized by delicate manipulation of the synthesis condition involved in nucleation and growth processes, including reaction temperature, solvent composition, and capping ligands.

Meanwhile, rational doping of RE ions in UCNPs has been found as an effective way to control the particle size. Liu and co-workers have proved that the ionic radii of RE could efficiently affect the growth of UCNPs (Figure 1).[13] The density functional theory calculations revealed an increase in the surface charge density of $NaYF_4$ NPs when Gd^{3+} is doped, slowing the diffusion of F^- ions onto the particle surface, thus altering the growth process. An increase in UC emission intensity is also observed with structure transition to a hexagonal one. Wang and co-workers introduced 14 lanthanides as dopants in $NaYF_4$ nanorods,[14] and a prominent tendency in size was elucidated as the ionic radii increased. Li and co-workers found that the doping of Gd^{3+} not only induced hexagonal NPs other thane cubic ones but also helped to reduce the size to 7.8 nm simultaneously.[15] It is noteworthy that these $NaLuF_4$-based UCNPs showed an intense UC emission, which is 1 order of magnitude higher than their 20 nm $NaYF_4$-based counterpart, which could be attributed to the similar ionic radii between Lu^{3+} and Yb^{3+}/Er^{3+} ions.

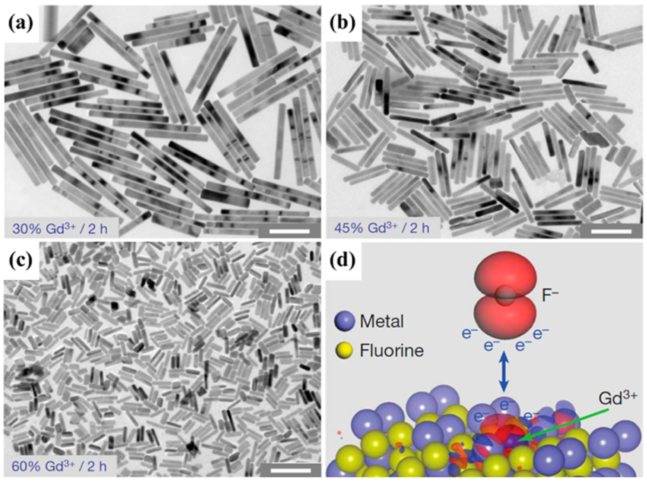

Figure 1. Size decrease of $NaYF_4$:Gd,Yb,Er nanorods induced by Gd^{3+} doping. (a–c) TEM images of $NaYF_4$:Yb,Er,Gd NPs. (d) Mechanism of particle size reduction. Reproduced with permission from reference 13. Copyright Nature Publishing Group 2010.

Besides the ionic radii, the valence of the cations could also efficiently affect the growth of UCNPs.[16] In this case, the introduction of trivalent RE ions to divalent alkaline earth fluorides results in a similar surface charge modulation effect. While the undoped SrF_2 NPs showed various morphology and a broad size distribution, 20% doping of La^{3+} ions effectively diminished the large NPs and decreased the average size to sub-5 nm, with high monodispersity.

2.2. Core/Shell-Structured Small UCNPs

With a higher proportion of RE ions near the surfaces, UC emission from NPs is sensitive to surface quenchers. Most importantly, with the NPs transferred from organic to aqueous phase, the hydrophobic ligands are often removed, resulting in

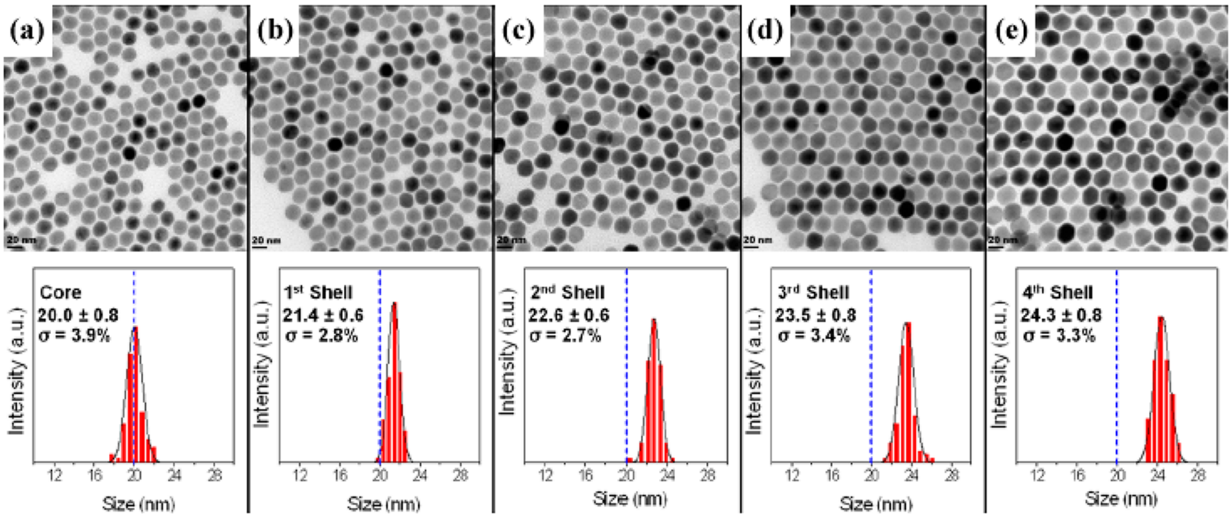

Figure 2. Continuous particle size tuning realized by multishell overgrowth. Reproduced with permission from reference 21. Copyright American Chemical Society 2012.

uncapped defects and adsorption of −OH groups, which act as strong quenchers to UC emissions.[17] In this case, energy dissipation is significant, and small NPs with relatively large surface area typically have a higher quenching probability. This imposes a challenge for small UCNPs in in vivo applications. Facing the above problems, minimizing the surface defects and protecting the nanoparticles from surface quenchers are critically considered.

To address the dilemma between particle size and surface quenching, core/shell nanostructures are designed for UCNPs. Generally, an undoped shell with a sufficient thickness could spatially isolate the luminescent centers from the surface quenchers, hence greatly reduce the quenching events. For UCNPs, an "inert" shell layer would inhibit the energy transfer from sensitizer and activator ions to surface quenchers and eventually increase the UC emission intensity.[18] As shown by Haase and co-workers, with a very limited increase in particle size (from 13 to 15.5 nm), the formation of undoped KYF_4 shell onto KYF_4:Yb,Er NPs leads to a greater than 20 times enhancement in UC emission.[19] In contrast to inert shells, as antennas of NIR light, Yb^{3+}-doped shells could further elevate UC emission, as has been reported by Capobianco and co-workers.[20] The core/shell structure also offers a facile toolkit to tune the particle size continuously (Figure 2),[21] by which consistent enhancement in UC emission intensity was observed as expected.

Recently, Yan and co-workers designed a novel type of heterogeneous core/shell-structured UCNPs, $NaYF_4$:Yb,Er/Tm@CaF_2 (Figure 3).[22] With the benefit from a small lattice mismatch between cubic-phase $NaYF_4$ and CaF_2, the core/shell structure was constructed by the epitaxial growth method. The mean particle size could be tuned from ≈9 to 13 nm with various CaF_2 shell thicknesses. A 300 times enhancement of UC emission was observed, and only trace amounts of RE ions were detected with dialysis. Compared to NPs with surface-exposed RE ions, the shell without RE doping could diminish the potential biotoxicity risk from RE ions.[23] This strategy has been later adopted by Han and co-workers in $NaLnF_4$:Yb,Tm@CaF_2 NPs as strong emitters for deep-tissue in vivo imaging and photoactivation studies.[24,25]

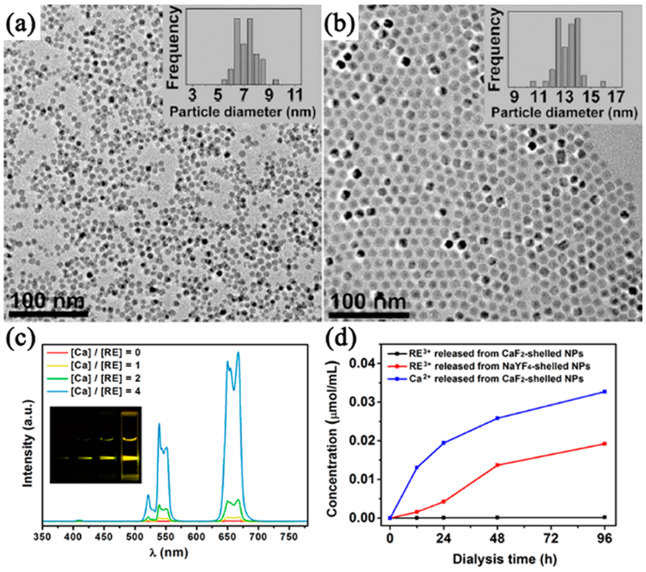

Figure 3. TEM images of $NaYF_4$:Yb,Er (a) and $NaYF_4$:Yb,Er@CaF_2 (b) NPs, the UC emission spectra with great enhancement (c), and ion release profile (d). Reproduced with permission from reference 22. Copyright Wiley-VCH 2012.

3. TUNING THE EMISSION AND EXCITATION OF UCNPS

3.1. Emission Profile Affected by Size, Morphology, and Doping

Although the UC emission wavelengths are strictly limited by the electronic manifolds of the dopants, the spectral profile could be variable with many factors. It is noteworthy that there is no universally "favorable" spectral profile, instead, it depends on the proposed applications. For deep-tissue imaging, NIR or red emission are preferred as they are less absorbed by animal tissue. On the contrary, UV or blue photons are expected to trigger photochemical reactions. Single-band emission with high color purity would be ideal in multicolor imaging applications; however, two ratiometric emission bands are good for sensing and detection studies.

The structure, size, and crystallization show complex effects on the spectral character of UCNPs. By changing these factors, multiple aspects in the UC process could be influenced, including the surface and internal defects, photon relaxation probability, and energy transfer scheme between the dopants. However, these parameters significantly depend on the synthesis, which makes it difficult to compare among different reports. Several reports observed a red-to-green ratio increase with decreasing size of UCNPs (Figure 4).[26,27] On the contrary, a decrease of red-to-green ratio with decreasing size is also reported.[28] It is difficulty to continuously and independently vary the structure and size challenges of the f—f transition assessments and color-tuning ability for UCNPs obtained with different synthetic methods.

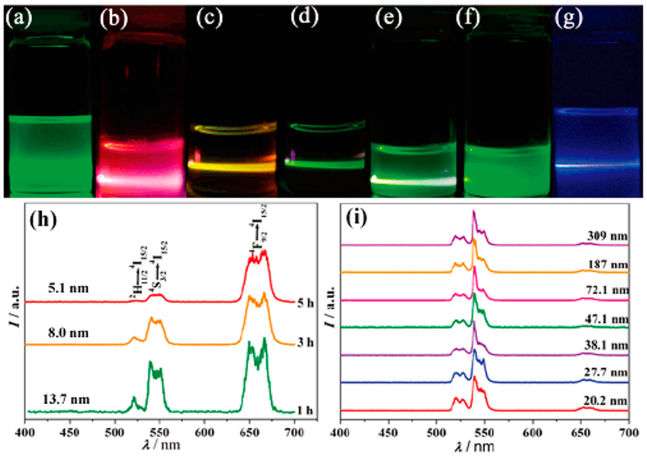

Figure 4. UC emission color tuned by doping concentration and particle size. Reproduced with permission from reference 18. Copyright American Chemical Society 2007.

Many earlier works have been focused on the color tuning by varying the composition and dopants. Yan and co-workers have earlier demonstrated this for $NaYF_4$:Yb,Er/Tm UCNPs.[18,29] A systemic research on this effect is reported by Wang and Liu in Yb/Er/Tm-codoped UCNPs.[30] Nonetheless, only a few activators (Er^{3+}, Tm^{3+}, and Ho^{3+} in most cases) are efficient in the $Yb^{3+}\rightarrow$activator energy transfer route, which limits the available UC emission color to a small part of the UV—vis—NIR region. A strategy to overcome this bottleneck is introduced by Liu and co-workers (Figure 5).[31] In their design named energy migration upconversion (EMU), the excitation energy is accumulated by a $Yb^{3+}\rightarrow Tm^{3+}$ UC process in the cores, followed by energy transfer from Tm^{3+} ($^1I_6$) to Gd^{3+} ($^6P_{7/2}$) and further to X^{3+} ($Eu^{3+}/Tb^{3+}/Sm^{3+}/Dy^{3+}$) in shells, resulting in their respective emissions. Furthermore, the emission from X^{3+} could be enhanced by building an extra inert shell on the UCNPs, which makes EMU a dominant destination of the energy transfer pathway.[32]

As there is little interference between transitions of RE ions, it is also practical to achieve tunable multicolor emission on a larger scale through self-assembly of NPs with different dopants and, consequently, different UC emission profiles. Yan and co-workers reported a bilayer assembly of UCNPs with a $NaYF_4$:Yb,Tm@CaF_2 layer and a $NaYF_4$:Yb,Er layer,[33] in which the emission intensities of the crossed region showed simple additivity of the constituent monolayers.

3.2. Single-Band Emission of UCNPs

Another attempt in UC emission color tuning is to achieve single-band emission. The abundant $4f^N$ electronic states endowed UCNPs with multiple transitions under a single-wavelength excitation. However, the multiple transitions from different RE ions could cause interference in in vivo detection. The deep red or NIR emission is less absorbed and scattered by tissues, and this fact makes it desirable to obtain highly pure red or NIR UC emission for in vivo imaging. As the NIR emission is usually dominant in Yb^{3+},Tm^{3+}-doped UCNPs, many efforts have been devoted to single-band red emission from Yb^{3+},Er^{3+}-doped UCNPs.

Generally, single-band emission can be achieved by controlling the equilibrium between different excited states or by filtering one or more unwanted emission bands. The first strategy involves changes in the energy transfer pathway in the UC process. Liu and co-workers reported a pure red emission from $KMnF_3$:Yb,Er (Figure 6a) NPs.[34] The $Er^{3+}\rightarrow Mn^{2+}$ energy transfer led to depopulation of green-emitting $^2H_{11/2}$ and $^4S_{3/2}$ manifolds, and the consequent $Mn^{2+}\rightarrow Er^{3+}$ back energy transfer populates the red-emission-participating $^4I_{13/2}$ and $^4F_{9/2}$ manifolds. Similarly, the doping of Ce^{3+} in $NaYF_4$:Yb,Ho NPs was reported to increase the red-to-green ratio with energy

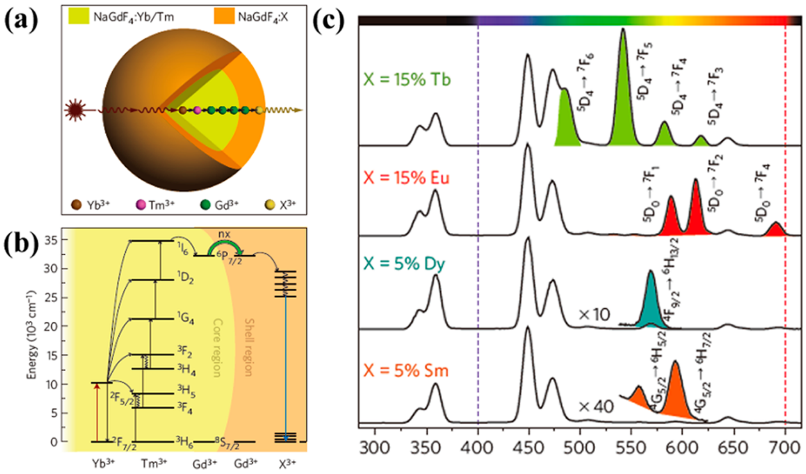

Figure 5. EMU mechanism (a,b) and the resultant UC emission spectra (c). Reproduced with permission from reference 31. Copyright Nature Publishing Group 2011.

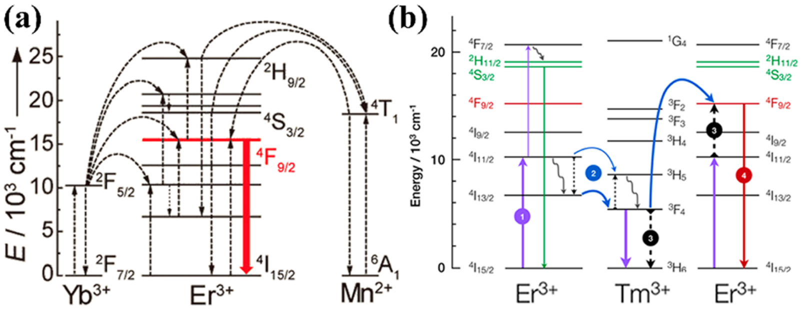

Figure 6. Mechanism of single-band UC emission realized by modulation of energy transfer pathway in (a) KMnF$_3$:Yb,Er NPs. Reproduced with permission from reference 34. Copyright Wiley-VCH 2011. (b) NaYF$_4$:Er,Tm NPs. Reproduced with permission from reference 36. Copyright American Chemical Society 2012.

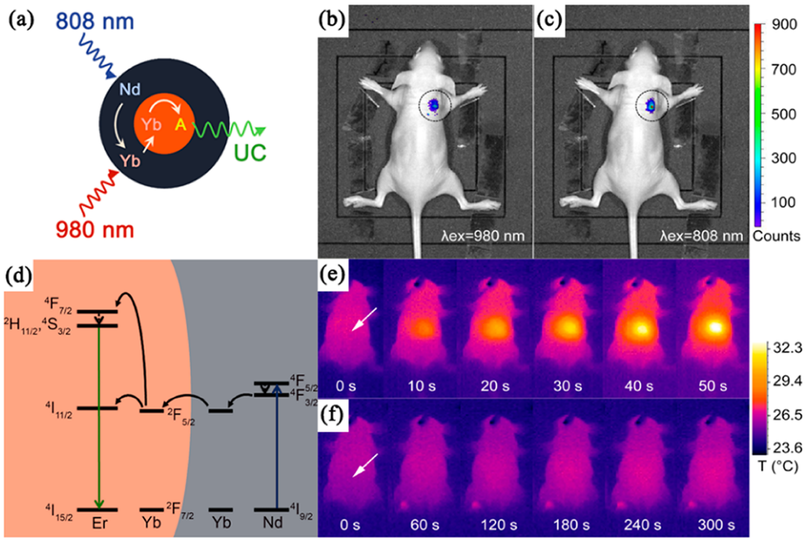

Figure 7. Excitation wavelength shifting realized by the Nd^{3+}-sensitized UC process. Reproduced with permission from reference 47. Copyright American Chemical Society 2013.

transfer between Ho^{3+} and Ce^{3+}.[35] More recently, Milliron and co-workers reported research on tuning UC emission color purity by binary or triple RE ion doping.[36] The Er^{3+}/Tm^{3+} pair showed that a pure red emission (Figure 6b) arose from the Er^{3+}→Tm^{3+} energy transfer, which populates the $^3F_4$ state of Tm^{3+} and eventually the $^4F_{9/2}$ state of Er^{3+}.

The other way to achieve single-band UC emission is to tailor the emission spectra by introducing external absorbers, quenchers, or other energy-transfer donors. Yan and co-workers have earlier tuned the emission color of UCNPs by embedding them into photonic crystal with a photonic band gap at 545 nm,[37] which filtered the green emission band. As the SPR bands of Au NPs could be reversibly shifted by pH-controlled assembly, they are used as absorbers to tune the red-to-green emission ratio.[38] The similar concept was also illustrated in a compact NaYF$_4$:Yb,Er@SiO$_2$@Au nanostructure,[39] with the SPR band tuned by the interparticle distance of Au NPs.

Moreover, fluorescence resonance energy transfer (FRET) acceptors could serve as internal filters. Wolfbeis and co-workers conjugated dye molecules with different absorption profiles onto UCNPs,[40] in which the dye molecules could selectively "screen off" part of one emission band. Branda and co-workers decorated UCNPs with a photochromic molecule whose absorption overlaps with the green UC emission,[41] and the UC emission color could thus be external light irradiation. Similarly, by covalently conjugating photochromic spiropyran molecules, Yan and co-workers reported the reversible switching of green emission of dual-emissive UCNPs.[42] The possibility to obtain an arbitrary intensity ratio between different emission bands through quantitative filtering and switching make UCNPs flexible in various applications.

3.3. Excitation Wavelength Tuning

Despite the progress in emission color tuning, the excitation wavelength of UC process has been limited to 980 nm (Yb^{3+}, $^2F_{7/2}$→$^2F_{5/2}$). The motive to modify UC excitation comes from two aspects: to broaden the excitation band for efficient conversion of NIR light from sunlight and to minimize water absorption and the local heating effect for in vivo studies.[43]

As dye molecules show much broader absorption bands and larger absorption cross sections compared with RE ions, NIR dye molecules are the first choice as antennas to broaden and enhance the excitation of UCNPs.[44] As reported by Hummelen and co-workers, NIR dyes could enable the excitation of UCNP across a much broader wavelength range, 720−1000 nm. Benefiting from the sensitizing and increased absorptivity, the overall upconversion efficiency is further enhanced by over 3000 times.

Other attempts were also reported to select the absorptions other than 980 nm, as shown by He and co-workers.[45] By utilizing the absorption of Yb^{3+} at 915 nm with less water absorption, the tissue overheating effect was suppressed. Prasad

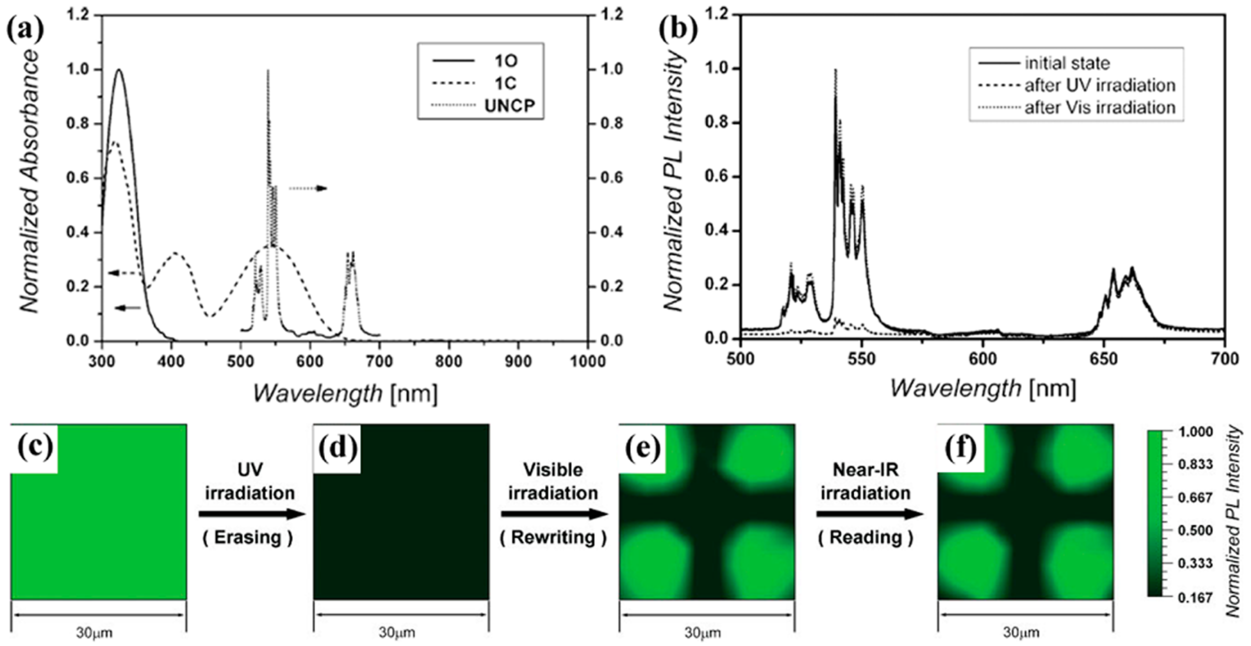

Figure 8. Nondestructive data readout supported by the composite of UCNPs and photochromes. Reproduced with permission from reference 61. Copyright Wiley-VCH 2010.

and co-workers employed the absorption of Er^{3+} at around 1490 nm to shift the UC excitation to longer NIR wavelength, by which emissions from two- and multiphoton UC processes were observed.[46]

Recently, Yan and co-workers proposed a new route to shift the excitation band of UCNPs (Figure 7).[47] An energy transfer route as $Nd^{3+} \rightarrow Yb^{3+} \rightarrow Er^{3+}$ was constructed in $NaGdF_4$:Yb,Er@$NaGdF_4$:Nd,Yb nanostructures. With a large absorption cross section of Nd^{3+} at 808 nm, a similar UC excitation efficiency to that of 980 nm was demonstrated. Meanwhile, as the water absorption at 808 nm is less than 1/20 of that at 980 nm, the laser-induced tissue heating effect was minimized. Han and co-workers realized cascaded-sensitized 800 nm excitable UC emission in Nd-doped UCNPs,[48] and the mechanism and applications of these Nd^{3+}-sensitized UC process were well-studied recently by Liu and Wang et al.[49,50] These advantages make Nd^{3+}-sensitized UCNPs appropriate for in vivo applications, especially in which long-duration and high power-density irradiation is required, such as NIR-light-triggered drug release or photodynamic therapy. It is also of great interest to employ these NPs as dual-mode probes, which respond both in NIR-to-visible mode and NIR-to-NIR mode.[51]

4. APPLICATIONS OF COLOR-TUNABLE UCNPS

During the past few years, considerable work has been done to demonstrate the potential of UCNPs as in vivo imaging probes for small animals. For readers who are interested, a dedicated review article on this topic which was recently published is recommended.[52] In this section, we will mainly focus on several typical applications, including in vivo multicolor imaging, detection and sensing, and UCNPs as light converters.

4.1. In Vivo Multicolor UC Imaging

Multicolor imaging is of great interest as it allows simultaneous tracing of different biochemical species and monitoring of multiple organs. As UCNPs generate distinct narrow emissions, they are expected to act as good probes for multicolor imaging. A demonstration of this idea is shown by Tian and co-workers[53] for UCNPs with different dopants, including Yb/Tm, Yb/Ho/Ce, and Yb/Ho. The development of a spectral deconvolution method also enables the utilization of multiplexed spectral features, which increases the available color channels for multicolor imaging, as shown by Liu and co-workers using dye-modified UCNPs.[54] After spectral unmixing, five-color imaging in a nude mouse was achieved.

For deeper-tissue in vivo imaging, the multiplexed spectral information may be lost during penetration. However, it is possible to obtain the depth information from spectral change of the in vivo probes.[14] If the inhomogeneity of tissue absorption and scattering could be considered and the modeling is realized, this technique would be useful in depth-sensitive “3D” in vivo imaging.

4.2. UC-Based Sensing and Detection

The anti-Stokes shift of the UC process and the low background luminescence interference along with the high photostability makes UCNPs promising probes in sensing and detection applications. Generally, the UC luminescence intensity is correlated to the concentration of analytes in either “turn-off” or “turn-on” mode.

The UCNPs could be recognized and immobilized by immunoreaction and DNA hybridization with the analytes,[55] and the concentration of analytes could be read out from changes in emission intensity directly. However, if only the emission wavelength is distinguished, the detection channels would be limited to a few. Actually, the relative emission intensity from different transition wavelength could also be used as a detectable index, and this idea has expedited the concept of color-coding for UCNPs.[7,56]

The “turn-on” or “turn-off” mode could be realized in either a simple emission-reabsorption scheme (inner filter effect) or a distance-restricted LRET process. For example, Li and co-workers reported the LRET-based detection for cyanide (CN^-) ions,[57] in which the green UC emission quenched by iridium complexes would be recovered when adding CN^-. In a different design, Zhang and co-workers reported a signal-amplifiable

DNA detection method,[58] where the target DNA "catalyzed" the trapping reaction of quencher to UCNPs. Li and co-workers also designed dye-modified $NaYF_4$:Yb,Er,Tm NPs for detection of $MeHg^+$ ions.[59] Upon the recognition, the absorption band of dye shifts from red to NIR, resulting in simultaneous "turn on" and "turn off" of different UC emission bands.

4.3. UCNPs as Remote Light Converters

Besides being detected and recorded directly (imaging or sensing), the UC emission could also be utilized to trigger photochemical reactions. In this case, UCNPs serve as an "internal" light source, switched by NIR light remotely.[60] Compared with "external" UV/vis irradiation, the UCNPs could offer higher penetration depth, promote the spatial specificity, and minimize damage or interference.

Yan and co-workers demonstrated this concept by constructing a 2D rewritable storage device based on green-emitting UCNPs and a photochromic molecules atop layer (Figure 8),[61] which realized nondestructive data reading. Yu and co-workers introduced $NaYF_4$:Yb,Tm NPs into azotolane-containing liquid crystal molecules,[62] and the trans−cis photoisomerization of the azotolane units could be rapidly triggered by the incident NIR light.

An emerging research interest in photodynamic therapy (PDT) is to activate with UC emissions.[63] Visible UC emissions could stimulate photosensitizers to produce toxic singlet oxygen ($^1O_2$) and serves in in vivo imaging as well. Yan and co-workers have built a triple-functional UCNPs with $NaGdF_4$:Yb,Er@CaF_2@SiO_2 structures,[64] in which the photosensitizers are loaded in the silica shells. These NPs could be used as UC/MRI dual-modal imaging probes and NIR light-activated PDT agents simultaneously.

Another typical photochemical process is photocleavage, which enables photocontrolled drug release. Five-photon upconverted emission from Yb^{3+}/Tm^{3+}-codoped NPs is especially attractive to convert NIR irradiation to UV light. Liu and co-workers reported in vivo "uncaging" of D-luciferin with $NaYF_4$:Yb,Tm NPs, and the resulting bioluminescence was also observed.[65] Zhang and co-workers reported the NIR-light-triggered release of DNA and siRNA molecules beneath deep tissues with the help of $NaYF_4$:Yb,Tm NPs.[66] It should be noted that the success of an "internal" light source idea relies on the emission intensity from the UCNPs. UC emission intense enough for in vivo imaging may be not intense enough to trigger a photochemical reaction, and this aspect may explain why less work carried out in deep tissue. The prospect of targeted therapy or delivery in vivo has posed a challenge on obtaining UCNPs with higher quantum efficiency.

5. CONCLUDING REMARKS

In this Account, we offered a glimpse of the recent development in tuning emission/excitation spectra and improving the upconversion luminescence for RE-ion-doped UCNPs. Different designs which either introduce dopants to modulate the growth thermodynamics or employ a shell layer to prevent energy loss in UC process have been proved to be successful in obtaining small NPs with high UC emission intensity. Furthermore, various studies have shown that UC excitation and emission spectral profiles can be tuned by alternating the size, structure, doping level of sensitizer/activator ions, and conjugated molecules/NPs. Rational design of energy transfer in the UC process has been realized by introducing transition metal−RE ion interactions and core/shell-structure-based EMU. Either multiplexed or purified single-band emission has been achieved and employed in different applications.

To further understand and utilize the unique luminescence properties of UCNPs, there are still many questions yet to be answered. For example, it is important to fabricate efficient UCNPs, which would not only benefit the imaging and photoactivated reactions but also alleviate the laser-induced damages. It would be also helpful to investigate the UC emission spectral profile changes when conjugated with biomolecules, considering the applications in complex in vivo environment for quantitative sensing and imaging. We believe that the design and analysis of complicated UC nanostructures/nanocomposites would lead to an extended research and application field for UCNPs.

AUTHOR INFORMATION

Funding

This research was supported by NSFC (Nos. 20971005 and 20931160429) and MOST of China (No. 2011AA03A407).

Notes

The authors declare no competing financial interest.

Biographies

Ling-Dong Sun was born in Heilongjiang, China, in 1969. She received her PhD from Changchun Institute of Physics, CAS in 1996. After her postdoctoral research, she became Lecturer (1998), Associate Professor (1999), and Professor (2011) of Peking University. Her research fields are rare earth and semiconductor functional nanomaterials.

Ye-Fu Wang was born in Fuzhou, China, in 1987. He received his BS degree in Chemistry from Peking University in 2009, then he joined the research group of Professor Chun-Hua Yan as a PhD student. His research interests are focused on the design and biological applications of rare earth luminescent nanomaterials.

Chun-Hua Yan was born in Shanghai, China, in 1961. He received his PhD from Peking University (PKU) in 1988. He later became Lecturer (1988), Associate Professor (1989), Professor (1992), and Cheung Kong Professor of Chemistry (1999). He became a Member of the Chinese Academy of Sciences in 2011 and a Fellow of TWAS in 2012. His research fields are rare earth functional materials and molecular based materials.

REFERENCES

(1) Wang, F.; Liu, X. Recent Advances in the Chemistry of Lanthanide-Doped Upconversion Nanocrystals. *Chem. Soc. Rev.* **2009**, *38*, 976−989.

(2) Auzel, F. Upconversion and Anti-Stokes Processes with f and d Ions in Solids. *Chem. Rev.* **2004**, *104*, 139−174.

(3) Haase, M.; Schäfer, H. Upconverting Nanoparticles. *Angew. Chem., Int. Ed.* **2011**, *50*, 5808−5829.

(4) Wang, M.; Abbineni, G.; Clevenger, A.; Mao, C.; Xu, S. Upconversion Nanoparticles: Synthesis, Surface Modification and Biological Applications. *Nanomedicine: Nanotechnol. Biol. Med.* **2011**, *7*, 710−729.

(5) Fragioni, J. V. In Vivo Near-Infrared Imaging. *Curr. Opin. Chem. Biol.* **2003**, *7*, 626−634.

(6) Yang, T.; Sun, Y.; Liu, Q.; Feng, W.; Yang, P.; Li, F. Cubic Sub-20 nm $NaLuF_4$-Based Upconversion Nanophosphors for High-Contrast Bioimaging in Different Animal Species. *Biomaterials* **2012**, *33*, 3733−3742.

(7) Zhang, F.; Shi, Q. H.; Zhang, Y.; Shi, Y.; Ding, K.; Zhao, D.; Stucky, G. D. Fluorescence Upconversion Microbarcodes for Multiplexed Biological Detection: Nucleic acid Encoding. *Adv. Mater.* **2011**, *23*, 3775−3779.

(8) Xiong, L.; Yang, T.; Yang, Y.; Xu, C.; Li, F. Long-Term In Vivo Biodistribution Imaging and Toxicity of Polyacrylic Acid-Coated Upconversion Nanophosphors. *Biomaterials* **2010**, *31*, 7078−7085.

(9) Zhou, J. C.; Yang, Z. L.; Dong, W.; Tang, R. J.; Sun, L. D.; Yan, C. H. Bioimaging and Toxicity Assessments of Near-infrared Upconversion Luminescent $NaYF_4$:Yb,Tm Nanocrystals. *Biomaterials* **2011**, *32*, 9059−9067.

(10) Dong, C.; Raudsepp, M.; van Veggel, F. C. J. M. Kinetically Determined Crystal Structures of Undoped and La^{3+}-Doped LnF_3. *J. Phys. Chem. C* **2009**, *113*, 472−478.

(11) Chen, G.; Qiu, H.; Fan, R.; Hao, S.; Tan, S.; Yang, C.; Han, G. Lanthanide-Doped Ultrasmall Yttrium Fluoride Nanoparticles with Enhanced Multicolor Upconversion Photoluminescence. *J. Mater. Chem.* **2012**, *22*, 20190−20196.

(12) Ostrowski, A. D.; Chan, E. M.; Gargas, D. J.; Katz, E. M.; Han, G.; Shuck, P. J.; Milliron, D. J.; Cohen, B. E. Controlled Synthesis and Single-Particle Imaging of Bright, Sub-10 nm Lanthanide-Doped Upconverting Nanocrystals. *ACS Nano* **2012**, *6*, 2686−2692.

(13) Wang, F.; Han, Y.; Lim, C. S.; Lu, Y.; Wang, J.; Xu, J.; Chen, H.; Zhang, C.; Hong, M.; Liu, X. Simultaneous Phase and Size Control of Upconversion Nanocrystals through Lanthanide Doping. *Nature* **2010**, *463*, 1061−1065.

(14) Yu, X.; Li, M.; Xie, M.; Chen, L.; Li, Y.; Wang, Q. Dopant-Controlled Synthesis of Water-Soluble Hexagonal $NaYF_4$ Nanorods with Efficient Upconversion Fluorescence for Multicolor Bioimaging. *Nano Res.* **2010**, *3*, 51−60.

(15) Liu, Q.; Sun, Y.; Yang, T.; Feng, W.; Li, C.; Li, F. Sub-10 nm Hexagonal Lanthanide-Doped $NaLuF_4$ Upconversion Nanocrystals for Sensitive Bioimaging In Vivo. *J. Am. Chem. Soc.* **2011**, *133*, 17122−17125.

(16) Chen, D.; Yu, Y.; Huang, F.; Huang, P.; Yang, A.; Wang, Y. Modifying the Size and Shape of Monodisperse Bifunctional Alkaline-Earth Fluoride Nanocrystals through Lanthanide Doping. *J. Am. Chem. Soc.* **2010**, *132*, 9976−9978.

(17) Bogdan, N.; Vetrone, F.; Ozin, G. A.; Capobianco, J. A. Synthesis of Ligand-Free Colloidally Stable Water Dispersible Brightly Luminescent Lanthanide-Doped Upconverting Nanoparticles. *Nano Lett.* **2011**, *11*, 835−840.

(18) Mai, H. X.; Zhang, Y. W.; Sun, L. D.; Yan, C. H. Highly Efficient Multicolor Up-Conversion Emissions and Their Mechanisms of Monodisperse $NaYF_4$:Yb,Er Core and Core/Shell-Structured Nanocrystals. *J. Phys. Chem. C* **2007**, *111*, 13721−13729.

(19) Schäfer, H.; Ptacek, P.; Zerzouf, O.; Haase, M. Synthesis and Optical Properties of KYF_4/Yb, Er Nanocrystals, and Their Surface Modification with Undoped KYF_4. *Adv. Funct. Mater.* **2008**, *18*, 2913−2918.

(20) Vetrone, F.; Naccache, R.; Mahalingam, V.; Morgan, C. G.; Capobianco, J. A. The Active-Core/Active-Shell Approach: A Strategy to Enhance the Upconversion Luminescence in Lanthanide-Doped Nanoparticles. *Adv. Funct. Mater.* **2009**, *19*, 2924−2929.

(21) Johnson, N. J. J.; Korinek, A.; Dong, C.; van Veggel, F. C. J. M. Self-Focusing by Ostwald Ripening: A Strategy for Layer-by-Layer Epitaxial Growth on Upconverting Nanocrystals. *J. Am. Chem. Soc.* **2012**, *134*, 11068−11071.

(22) Wang, Y. F.; Sun, L. D.; Xiao, J. W.; Feng, W.; Zhou, J. C.; Shen, J.; Yan, C. H. Rare-Earth Nanoparticles with Enhanced Upconversion Emission and Suppressed Rare-Earth-Ion Leakage. *Chem.—Eur. J.* **2012**, *18*, 5558−5564.

(23) Grobner, T. Gadolinium−A Specific Trigger for the Development of Nephrogenic Fibrosing Dermopathy and Nephrogenic Systemic Fibrosis? *Nephrol. Dial. Transplant.* **2006**, *21*, 1104−1108.

(24) Chen, G.; Shen, J.; Ohulchanskyy, T. Y.; Patel, N. J.; Kutikov, A.; Li, Z.; Song, J.; Pandey, R. K.; Ågren, H.; Prasad, P. N.; Han, G. (α-$NaYbF_4$:Tm^{3+})/CaF_2 Core/Shell Nanoparticles with Efficient Near-Infrared to Near-Infrared Upconversion for High-Contrast Deep Tissue Bioimaging. *ACS Nano* **2012**, *6*, 8280−8287.

(25) Shen, J.; Chen, G.; Ohulchanskyy, T. Y.; Kesseli, S. J.; Buchholz, S.; Li, Z.; Prasad, P. N.; Han, G. Upconversion: Tunable Near Infrared to Ultraviolet Upconversion Luminescence Enhancement in (α-$NaYF_4$:Yb,Tm)/CaF_2 Core/Shell Nanoparticles for In Situ Real-time Recorded Biocompatible Photoactivation. *Small* **2013**, *9*, 3213−3217.

(26) Mai, H. X.; Zhang, Y. W.; Si, R.; Yan, Z. G.; Sun, L. D.; You, L. P.; Yan, C. H. High-Quality Sodium Rare-Earth Fluoride Nanocrystals: Controlled Synthesis and Optical Properties. *J. Am. Chem. Soc.* **2006**, *128*, 6426−6436.

(27) Bai, X.; Song, H.; Pan, G.; Lei, Y.; Wang, T.; Ren, X.; Lu, S.; Dong, B.; Dai, Q.; Fan, L. Size-Dependent Upconversion Luminescence in Er^{3+}/Yb^{3+}-Codoped Nanocrystalline Yttria: Saturation and Thermal Effects. *J. Phys. Chem. C* **2007**, *111*, 13611−13617.

(28) Schietinger, S.; de S. Menezes, L.; Lauritzen, B.; Benson, O. Observation of Size Dependence in Multicolor Upconversion in Single Yb^{3+},Er^{3+} Codoped $NaYF_4$ Nanocrystals. *Nano Lett.* **2009**, *9*, 2477−2481.

(29) Yin, A. X.; Zhang, Y. W.; Sun, L. D.; Yan, C. H. Colloidal Synthesis and Blue Based Multicolor Upconversion Emissions of Size and Composition Controlled Monodisperse Hexagonal $NaYF_4$:Yb,Tm Nanocrystals. *Nanoscale* **2010**, *2*, 953−959.

(30) Wang, F.; Liu, X. Upconversion Multicolor Fine-Tuning: Visible to Near-Infrared Emission from Lanthanide-Doped $NaYF_4$ Nanoparticles. *J. Am. Chem. Soc.* **2008**, *130*, 5642−5643.

(31) Wang, F.; Deng, R.; Wang, J.; Wang, Q.; Han, Y.; Zhu, H.; Chen, X.; Liu, X. Tuning Upconversion Through Energy Migration in Core−Shell Nanoparticles. *Nat. Mater.* **2011**, *10*, 968−973.

(32) Su, Q.; Han, S.; Xie, X.; Zhu, H.; Chen, H.; Chen, C.; Liu, R.; Chen, X.; Wang, F.; Liu, X. The Effect of Surface Coating on Energy Migration-Mediated Upconversion. *J. Am. Chem. Soc.* **2012**, *134*, 20849−20857.

(33) Zheng, T.; Sun, L. D.; Zhou, J. C.; Feng, W.; Zhang, C.; Yan, C. H. Construction of $NaREF_4$-Based Binary and Bilayer Nanocrystal Assemblies. *Chem. Commun.* **2013**, *49*, 5799−5801.

(34) Wang, J.; Wang, F.; Wang, C.; Liu, Z.; Liu, X. Single-Band Upconversion Emission in Lanthanide-Doped $KMnF_3$ Nanocrystals. *Angew. Chem., Int. Ed.* **2011**, *50*, 10369−10372.

(35) Chen, G.; Liu, H.; Somesfalean, G.; Liang, H.; Zhang, Z. Upconversion Emission Tuning from Green to Red in Yb^{3+}/Ho^{3+}-Codoped $NaYF_4$ Nanocrystals by Tridoping with Ce^{3+} Ions. *Nanotechnology* **2009**, *20*, 385704.

(36) Chan, E. M.; Han, G.; Goldberg, J. D.; Gargas, D. J.; Ostrowski, A. D.; Schuck, P. J.; Cohen, B. E.; Milliron, D. J. Combinatorial Discovery of Lanthanide-Doped Nanocrystals with Spectrally Pure Upconverted Emission. *Nano Lett.* **2012**, *12*, 3839−3845.

(37) Li, Z. X.; Li, L. L.; Zhou, H. P.; Yuan, Q.; Chen, C.; Sun, L. D.; Yan, C. H. Colour Modification Action of an Upconversion Photonic Crystal. *Chem. Commun.* **2009**, 6616−6618.

(38) Zhang, S. Z.; Sun, L. D.; Tian, H.; Liu, Y.; Wang, J. F.; Yan, C. H. Reversible Luminescence Switching of $NaYF_4$:Yb,Er Nanoparticles with Controlled Assembly of Gold Nanoparticles. *Chem. Commun.* **2009**, 2547−2549.

(39) Li, Z.; Wang, L.; Wang, Z.; Liu, X.; Xiong, Y. Modification of $NaYF_4$:Yb,Er@SiO_2 Nanoparticles with Gold Nanocrystals for Tunable Green-to-Red Upconversion Emissions. *J. Phys. Chem. C* **2011**, *115*, 3291−3296.

(40) Gorris, H. H.; Ali, R.; Saleh, S. M.; Wolfbeis, O. S. Tuning the Dual Emission of Photon-Upconverting Nanoparticles for Ratiometric Multiplexed Encoding. *Adv. Mater.* **2011**, *23*, 1652−1655.

(41) Boyer, J. C.; Carling, C. J.; Chua, S. Y.; Wilson, D.; Johnson, B.; Baillie, D.; Branda, N. R. Photomodulation of Fluorescent Upconverting Nanoparticle Markers in Live Organisms by Using Molecular Switches. *Chem.—Eur. J.* **2012**, *18*, 3122−3126.

(42) Zhang, C.; Xu, C. H.; Sun, L. D.; Yan, C. H. Photoswitchable Upconversion Luminescence of Rare-Earth Nanophosphors with Covalently Grafted Spiropyran. *Chem.—Asian. J.* **2012**, *7*, 2225−2229.

(43) Xie, X.; Liu, X. Photonics: Upconversion Goes Broadband. *Nat. Mater.* **2011**, *11*, 842−843.

(44) Zou, W.; Visser, C.; Maduro, J. A.; Pshenichnikov, M. S.; Hummelen, J. C. Broadband Dye-Sensitized Upconversion of Near-Infrared Light. *Nat. Photonics* **2012**, *6*, 560−564.

(45) Zhan, Q.; Qian, J.; Liang, H.; Somesfalean, G.; Wang, D.; He, S.; Zhang, Z.; Andersson-Engels, S. Using 915 nm Laser Excited $Tm^{3+}/Er^{3+}/Ho^{3+}$-Doped $NaYbF_4$ Upconversion Nanoparticles for In Vitro and Deeper In Vivo Bioimaging without Overheating Irradiation. *ACS Nano* **2011**, *5*, 3744−3757.

(46) Chen, G.; Ohulchanskyy, T. Y.; Kachynski, A.; Ågren, H.; Prasad, P. N. Intense Visible and Near-Infrared Upconversion Photoluminescence in Colloidal $LiYF_4:Er^{3+}$ Nanocrystals under Excitation at 1490 nm. *ACS Nano* **2011**, *5*, 4981−4986.

(47) Wang, Y. F.; Liu, G. Y.; Sun, L. D.; Xiao, J. W.; Zhou, J. C.; Yan, C. H. Nd^{3+}-Sensitized Upconversion Nanophosphors: Efficient In Vivo Bioimaging Probes with Minimized Heating Effect. *ACS Nano* **2013**, *7*, 7200−7206.

(48) Shen, J.; Chen, G.; Vu, A. M.; Fan, W.; Bilsel, O. S.; Chang, C. C.; Han, G. Engineering the Upconversion Nanoparticle Excitation Wavelength: Cascade Sensitization of Tri-Doped Upconversion Colloidal Nanoparticles at 800 nm. *Adv. Optical Mater.* **2013**, *1*, 644−650.

(49) Xie, X.; Gao, N.; Deng, R.; Sun, Q.; Xu, Q.; Liu, X. Mechanistic Investigation of Photon Upconversion in Nd^{3+}-Sensitized Core−Shell Nanoparticles. *J. Am. Chem. Soc.* **2013**, *135*, 12608−12611.

(50) Wen, H.; Zhu, H.; Chen, X.; Hung, T. F.; Wang, B.; Zhu, G.; Yu, S. F.; Wang, F. Upconverting Near-Infrared Light through Energy Management in Core−Shell−Shell Nanoparticles. *Angew. Chem., Int. Ed.* **2013**, DOI: 10.1002/anie.201306811.

(51) Rocha, U.; Kumar, K. U.; Jacinto, C.; Villa, I.; Sanz-Rodríguez, F.; de la Cruz, M. C. I.; Juarranz, A.; Carrasco, E.; van Veggel, F. C. J. M.; Bovero, E.; Solé, J. G.; Jaque, D. Neodymium-Doped LaF_3 Nanoparticles for Fluorescence Bioimaging in the Second Biological Window. *Small* **2013**, DOI: 10.1002/smll.201301716.

(52) Zhou, J.; Liu, Z.; Li, F. Upconversion Nanophosphors for Small-Animal Imaging. *Chem. Soc. Rev.* **2012**, *41*, 1323−1349.

(53) Tian, Z.; Chen, G.; Li, X.; Liang, H.; Li, Y.; Zhang, Z.; Tian, Y. Autofluorescence-Free In Vivo Multicolor Imaging Using Upconversion Fluoride Nanocrystals. *Lasers Med. Sci.* **2010**, *25*, 479−484.

(54) Cheng, L.; Yang, K.; Shao, M.; Lee, S.; Liu, Z. Multicolor In Vivo Imaging of Upconversion Nanoparticles with Emissions Tuned by Luminescence Resonance Energy Transfer. *J. Phys. Chem. C* **2011**, *115*, 2686−2692.

(55) Wu, S.; Duan, N.; Zhu, C.; Ma, X.; Wang, M.; Wang, Z. Magnetic Nanobead-Based Immunoassay for the Simultaneous Detection of Aflatoxin B1 and Ochratoxin A Using Upconversion Nanoparticles as Multicolor Labels. *Biosens. Bioelectron.* **2011**, *30*, 35−42.

(56) Gorris, H. H.; Wolfbeis, O. S. Optical Encoding and Multiplexing of Cells, Biomolecules and Microspheres using Photon-Upconverting Nanoparticles. *Angew. Chem., Int. Ed.* **2013**, *52*, 3584−3600.

(57) Liu, J.; Liu, Y.; Liu, Q.; Li, C.; Sun, L.; Li, F. Iridium(III) Complex-Coated Nanosystem for Ratiometric Upconversion Luminescence Bioimaging of Cyanide Anions. *J. Am. Chem. Soc.* **2011**, *133*, 15276−15279.

(58) Wang, P.; Ahmadov, T. O.; Lee, C.; Zhang, P. Ligase-Assisted Signal-Amplifiable DNA Detection Using Upconversion Nanoparticles. *RSC Adv.* **2013**, *3*, 16326−16329.

(59) Liu, Y.; Chen, M.; Cao, T.; Sun, Y.; Li, C.; Liu, Q.; Yang, T.; Yao, L.; Feng, W.; Li, F. A Cyanine-Modified Nanosystem for In Vivo Upconversion Luminescence Bioimaging of Methylmercury. *J. Am. Chem. Soc.* **2013**, *135*, 9869−9876.

(60) Carling, C. J.; Boyer, J. C.; Branda, N. R. Remote-Control Photoswitching Using NIR Light. *J. Am. Chem. Soc.* **2009**, *131*, 10838−10839.

(61) Zhang, C.; Zhou, H. P.; Liao, L. Y.; Feng, W.; Sun, W.; Li, Z. X.; Xu, C. H.; Fang, C. J.; Sun, L. D.; Zhang, Y. W.; Yan, C. H. Luminescence Modulation of Ordered Upconversion Nanopatterns by a Photochromic Diarylethene: Rewritable Optical Storage with Nondestructive Readout. *Adv. Mater.* **2010**, *22*, 633−637.

(62) Wei, W.; Yao, L.; Yang, T.; Yin, R.; Li, F.; Yu, Y. NIR-Light-Induced Deformation of Cross-Linked Liquid-Crystal Polymers Using Upconversion Nanophosphors. *J. Am. Chem. Soc.* **2011**, *133*, 15810−15813.

(63) Idris, N. M.; Gnanasammandhan, M. K.; Zhang, J.; Ho, P. C.; Mahendran, R.; Zhang, Y. In Vivo Photodynamic Therapy Using Upconversion Nanoparticles as Remote-Controlled Nanotransducers. *Nat. Med.* **2012**, *18*, 1580−1585.

(64) Qiao, X. F.; Zhou, J. C.; Xiao, J. W.; Wang, Y. F.; Sun, L. D.; Yan, C. H. Triple-Functional Core−Shell Structured Upconversion Luminescent Nanoparticles Covalently Grafted with Photosensitizer for Luminescent, Magnetic Resonance Imaging and Photodynamic Therapy In Vitro. *Nanoscale* **2012**, *4*, 4611−4623.

(65) Yang, Y.; Shao, Q.; Deng, R.; Wang, C.; Teng, X.; Cheng, K.; Cheng, Z.; Huang, L.; Liu, Z.; Liu, X.; Xing, B. In Vitro and In Vivo Uncaging and Bioluminescence Imaging by Using Photocaged Upconversion Nanoparticles. *Angew. Chem., Int. Ed.* **2012**, *51*, 3125−3129.

(66) Jayakumar, M. K. G.; Idris, N. M.; Zhang, Y. Remote Activation of Biomolecules in Deep Tissues Using Near-Infrared-to-UV Upconversion Nanotransducers. *Proc. Natl. Acad. Sci. U.S.A.* **2012**, *109*, 8483−8488.